NUMERICAL ANALYSIS OF THERMAL PERFORMANCE OF LATENT THERMAL ENERGY STORAGE SYSTEM USING SPIRAL COILS WITH VARIATIONS IN GEOMETRY AND TYPE OF PHASE CHANGE MATERIAL (PCM)

Taufan Firdhaus[1*], **Budhi M. Suyitno**[2]
[1,2]*Magister Teknik Mesin, Universitas Pancasila, Jakarta, Indonesia*
**Email Corresponding Author: taufanfirdhaus@gmail.com*

ABSTRAK

Penelitian ini menganalisis kinerja *Thermal Energy Storage* (TES) laten berbasis *Phase Change Material* (PCM) pada *shell-and-spiral heat exchanger* dengan variasi geometri saluran fluida dingin dan jenis PCM. Masalah utama sistem TES berbasis PCM adalah rendahnya konduktivitas termal yang memperlambat pelelehan dan menurunkan keseragaman temperatur. Simulasi numerik dilakukan menggunakan *Computational Fluid Dynamics* dengan pendekatan *enthalpy-porosity* pada dua konfigurasi, yaitu Geometri 1 dengan satu pipa CTF berdiameter besar dan Geometri 2 dengan lima pipa CTF berdiameter kecil. PCM yang dikaji adalah *Paraffin Wax* dan Eritritol, sedangkan temperatur *inlet* HTF divariasikan pada 130, 150, dan 170 °C dengan kecepatan 1-3 m/s. Hasil menunjukkan bahwa Geometri 2 memperbaiki distribusi temperatur, mempercepat perkembangan fraksi cair, dan meningkatkan efektivitas transfer panas. Waktu leleh minimum *Paraffin Wax* menurun dari 480 s pada Geometri 1 menjadi 180 s pada Geometri 2, sedangkan Eritritol menurun dari 1740 s menjadi 1560 s. Energi tersimpan terutama dipengaruhi jenis PCM dan temperatur operasi, bukan konfigurasi geometri. Geometri *multi-CTF* direkomendasikan untuk TES yang membutuhkan respons termal cepat dan distribusi panas merata.

Kata kunci: CFD; *enthalpy-porosity*; *Phase Change Material*; *shell-and-spiral heat exchanger*; *Thermal Energy Storage*.

ABSTRACT

This study investigates the performance of a Phase Change Material (PCM)-based latent Thermal Energy Storage (TES) system integrated with a shell-and-spiral heat exchanger under variations in cold transfer fluid channel geometry and PCM type. The key limitation of PCM-based TES is low thermal conductivity, which slows melting and reduces temperature uniformity. A Computational Fluid Dynamics simulation using the enthalpy-porosity approach was conducted for two configurations: Geometry 1 with one large CTF pipe and Geometry 2 with five smaller CTF pipes. Paraffin Wax and Erythritol were evaluated at HTF inlet temperatures of 130, 150, and 170 °C and velocities of 1-3 m/s. The results show that Geometry 2 improves temperature distribution, accelerates liquid-fraction development, and enhances heat-transfer effectiveness. The minimum melting time of Paraffin Wax decreased from 480 s in Geometry 1 to 180 s in Geometry 2, while Erythritol decreased from 1740 s to 1560 s. Stored energy was governed mainly by PCM type and operating temperature rather than geometry. The multi-CTF configuration is recommended for TES applications requiring rapid thermal response and uniform heat distribution.

Keywords: *CFD; enthalpy-porosity; Phase Change Material; shell-and-spiral heat exchanger; Thermal Energy Storage.*

INTRODUCTION

The mismatch between heat availability time and thermal load requirement time remains an important issue in modern energy systems. Latent heat-based *Thermal Energy Storage* (TES) offers a solution because it can store energy at high density within a relatively constant temperature range. However, *Phase Change Material* (PCM) generally has low thermal conductivity, causing *the charging* process to slow down, uneven temperature distribution, and storage capacity not being optimally utilized [1]-[4].

Various studies have developed strategies to improve heat transfer in TES, including the use of helical pipes, spiral geometry, fins, *multi-tubes*, nanofluids, and composite PCMs. Studies on spiral coils show that longer fluid paths and secondary flow fields can enhance mixing and improve temperature uniformity [8], [10], [17]. Multi-tube research on *latent heat storage* also showed that adding contact surfaces can accelerate *charging* and *discharging* compared to *single tubes* [15].

The method currently widely used to evaluate PCM-based TES systems is *Computational Fluid Dynamics* (CFD) with *an enthalpy-porosity* model.

This method can predict temperature distribution, *liquid fraction*, and *mushy* zone dynamics without explicitly tracing the solid-liquid interface boundary [28], [31]. In spiral *heat exchanger design*, CFD is very useful because the flow distribution and three-dimensional geometry are difficult to observe experimentally.

Although spiral and *multi-tube* designs have been extensively studied, direct comparisons between *shell-and-spiral configurations* with one large CTF pipe and five small CTF pipes remain limited. Furthermore, the simultaneous influence of CTF geometry and two PCMs with different characteristics, namely *Paraffin Wax* and Erythritol, has not been widely reported. This gap is important because changes in the number of CTF pipes can alter heat propagation distance, thermal contact area, and *cold fluid* outlet response.

This study aims to analyze the thermal performance of latent TES on *shell-and-spiral heat exchangers* using two geometric configurations and two types of PCM through CFD simulation. The main contribution of this article is a comparative evaluation of temperature distribution, melting time, CTF outlet temperature, PCM efficiency, and stored energy, resulting in recommendations for more responsive and thermally uniform TES configurations.

Practically, this study is relevant for water heating systems, industrial waste heat utilization, and solar thermal energy integration that require compact storage units. The selection *of Paraffin Wax* and Erythritol also provides an overview of two different application needs: rapid response at medium temperatures and energy storage at higher temperatures. Therefore, this article not only compares numerical values but also interprets the design consequences on material selection and TES operational strategies.

RESEARCH METHOD

This research is a numerical study based on CFD with a quantitative approach. The research object is *a shell-and-spiral heat exchanger* consisting of a spiral pipe for *Heat Transfer Fluid* (HTF), a straight pipe for *Cold Transfer Fluid* (CTF), and PCM volume in the annulus chamber. Two geometries were compared: Geometry 1 uses one large-diameter CTF pipe at the center of the *shell*, while Geometry 2 uses five small CTF pipes consisting of one central pipe and four pipes around it.

Visualization of differences in CTF configuration is shown in Figure 1.

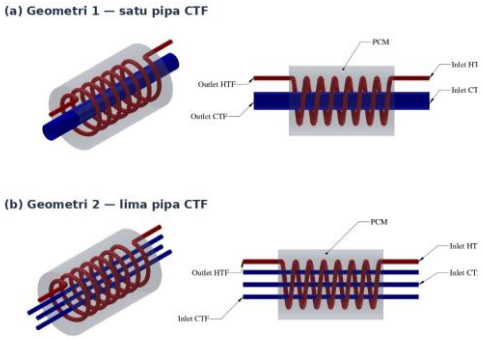


Figure 1. Shell-and-spiral model: (a) Geometry 1, (b) Geometry 2.

The PCM materials used are *Paraffin Wax* and Erythritol. *Paraffin Wax* represents low-to-medium-temperature organic PCM with a melting point of 56-58 °C and latent heat of 173.4 kJ/kg. Erythritol represents *a medium-high temperature sugar alcohol* with a melting point of about 119 °C and latent heat of 340 kJ/kg. HTF and CTF are modeled as water with thermophysical properties of temperature functions, while pipe walls are considered conductive and the outer shell is assumed adiabatic.

The research stages include literature study, 2D/3D geometry modeling, PCM selection, *mesh creation*, *solver setup*, validation, parameter variation simulation, data processing, and drawing conclusions. *The mesh* is constructed with *tetrahedral/polyhedral elements* and *an inflation layer* on the pipe walls. Mesh quality was evaluated through *skewness*, *orthogonal quality*, and *the Grid Independence Test*. The model was declared adequate if the change in inter-mesh results was within a small limit and the GCI index was below the 5% threshold.

The mesh formation results for Geometry 2 are shown in Figure 2.

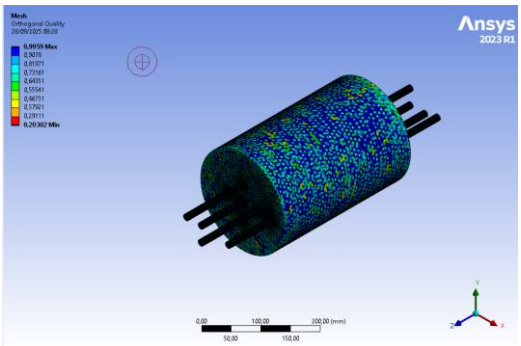


Figure 2. Numerical mesh in Geometry 2.

Simulations use *pressure-based transient solver*, *second-order upwind* schemes for momentum and energy, *implicit second-order* for time, and SIMPLE for *pressure-velocity coupling*. The standard k-epsilon turbulence model is used in the fluid domain to represent the spiral flow effect. PCM phase changes were calculated using *the enthalpy-porosity* model, with *liquid fractions* of 0 in the solid phase, 1 in the liquid phase, and 0-1 in the *mushy zone*.

The limit conditions are set as the *inlet velocity* on the HTF with temperatures of 130, 150, and 170 °C and velocities of 1, 2, and 3 m/s. The *outlet* side uses *a pressure outlet*, CTF has a constant *inlet* temperature, and the outer *shell wall is* assumed to have no heat loss. The total scenario is 36 combinations (2 geometries x 2 PCM x 3 temperature x 3 speeds). Evaluation parameters included temperature distribution, *liquid fraction*, *melting time*, CTF outlet temperature, PCM efficiency, and stored thermal energy.

The preprocessing stage begins with geometric simplification so that the simulated domain does not contain details that do not affect the main flow. All inter-domain wall connections are defined as *coupled walls* so that the heat transfer of conjugate between HTF, pipe wall, PCM, and CTF can be calculated simultaneously. This modeling is necessary because TES performance is determined not only by fluid convection but also by wall conduction resistance and PCM.

The basic equations solved include continuity, momentum, and energy. For the PCM domain, total enthalpy is expressed as the sum of sensitive and latent enthalpy. The liquid fraction increases from 0 to 1 according to the *solidus-liquid* temperature range. In the *mushy zone*, *a sink momentum* is applied so that the unmelted part of the PCM remains at flow resistance. This approach is commonly used for PCM because it can depict the stable movement of phase boundaries in a fixed grid.

The data collection procedure was carried out by exporting the average PCM temperature, temperature contour, *liquid fraction*, *CTF* outlet temperature, *heat flux*, and stored energy at certain time intervals until the PCM reaches a fully liquid state or the simulation reaches the final time. *Melting time* is defined as the time when the average *liquid fraction* approaches 1. PCM efficiency is calculated from the ratio of stored latent energy to the theoretical latent energy capacity of the material.

The research success parameters were set based on three indicators. First, shorter melting time indicates an increase *in charging* kinetics. Second, a higher and more stable CTF outlet temperature indicates the system's ability to transfer heat to the load. Third, PCM efficiency approaching 100% indicates that the energy received by the system is successfully utilized as latent heat storage. These three indicators are analyzed together so that design recommendations are not based on just one parameter.

Table 1. Simulation parameter design

Parameter	Description
Geometri	G1: 1 Big pipe CTF ; G2: 5 little pipe CTF
PCM	*Paraffin Wax* dan Eritritol
HTF Temperature	130, 150, dan 170 °C
HTF Speed	1, 2, dan 3 m/s
Model numerics	*Transient CFD*, *enthalpy-porosity*, k-epsilon
Indicator	Temperature distribution, *liquid fraction*, *melting time*, *outlet* CTF, PCM efficiency, stored energy

Table 2. Assumptions of physical and numerical models

Components	Main assumptions
Fluids HTF/CTF	*Incompressible*, *Newtonian*, temperature function properties
Pipe wall	Conduction, without thermal deformation
Outer shell	Adiabatic, environmental heat loss is ignored
PCM	Phase change with *enthalpy-porosity*
Solver	*Transient pressure-based*; *residual* momentum and energy <= 10^-4

Table 3. System performance evaluation formula

Quantity	Formulas and functions
Sensitive energy	Q = m Cp Delta T; measuring heat before/after phase change

Quantity	Formulas and functions
Latent energy	Q_L = m L; Measuring storage capacity during *melting*
CTF Temperature	Q = m_dot Cp (T_out - T_in); Assessing the heat received by cold fluids
PCM Efficiency	eta_PCM = Q_stored/(m_PCM L) x 100%; assess the effectiveness of latent storage

RESULTS AND DISCUSSION

Mesh verification showed that increasing the number of elements reduced *changes in outlet* temperature and melting time. *Fine mesh* was chosen because it provided stable results with changes within tolerance limits. Validation was conducted on the temperature pattern and melting mechanism of paraffin in the spiral coil study. The simulation results showed a consistent pattern, where heating started around the HTF pipe and then radially developed through natural conduction and convection. The alignment of these trends indicates that the model is feasible to compare geometric and PCM variations.

The tendency for error changes in the mesh independence test is shown in Figure 3.

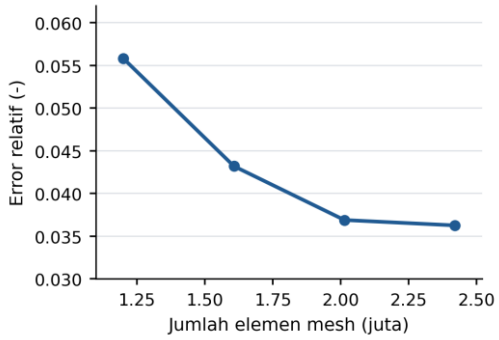


Figure 3. Mesh independence test graph

The temperature distribution shows a clear difference between the two geometries. In Geometry 1, heat flow from the spiral pipe to one large CTF pipe forms a centralized temperature gradient and a more uneven heat zone. In Geometry 2, the five CTF pipes divide the heat transfer path in several directions, shortening the conduction distance and expanding the thermal contact area. As a result, the temperature field becomes more homogeneous and *the mushy* zone develops more evenly.

An example of the temperature contours of both geometries under the same operating conditions is presented in Figure 4.

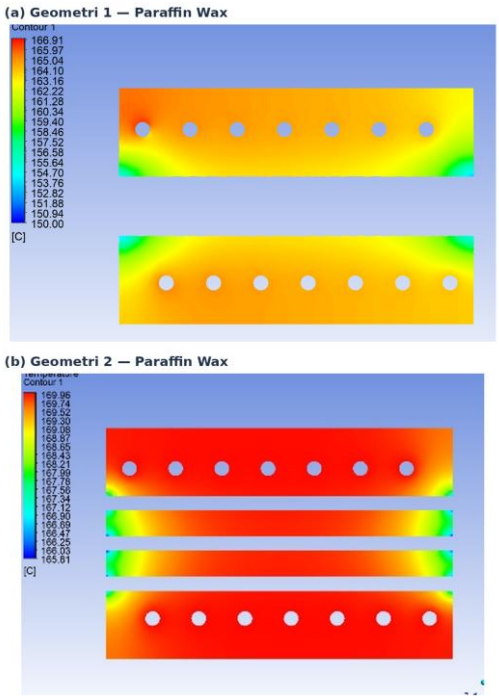


Figure 4. PCM Paraffin Wax Contour, 170 °C and 3 m/s: (a) G1, (b) G2

The type of PCM also affects thermal response. *Paraffin Wax* reaches melting temperature faster because its melting point is low, causing *the liquid fraction* to increase sharply at the start of the simulation. Erythritol requires greater sensitive and latent energy because its melting point and latent heat are higher. Thus, erythritol melts more slowly but shows good energy storage capacity and efficiency stability at high operating temperatures.

Table 4. PCM melting time

Conditions	Melting *time* results and interpretation
PW130	G1: 960 -> 780 s; G2: 720 -> 480 s; G2 descend 240-300 s
PW150	G1: 720 -> 600 s; G2: 540 -> 300 s; faster melting
PW170	G1: 720 -> 480 s; G2: 420 -> 180 s; minimum 180 s
ER130	G1: 3000 -> 2940 s; G2: 2580 -> 2520 s; small decline
ER150	G1: 2160 -> 2160 s; G2: 1980 -> 1860 s; stable yet slow

ER170	G1: 1800 -> 1740 s; G2: 1620 -> 1560 s; minimum 1560 s

Table 4 shows that Geometry 2 consistently shortens *melting time*. In *Paraffin Wax*, the minimum melting time drops from 480 s in Geometry 1 to 180 s in Geometry 2, equivalent to an acceleration of about 62.5%. For Erythritol, the minimum time drops from 1740 s to 1560 s, or about 10.3%. The difference in the magnitude of the increase shows that geometric modification is most effective when PCM has a low melting point and a fast melting response.

The comparison of melting time at HTF velocity of 3 m/s is shown in Figure 5.

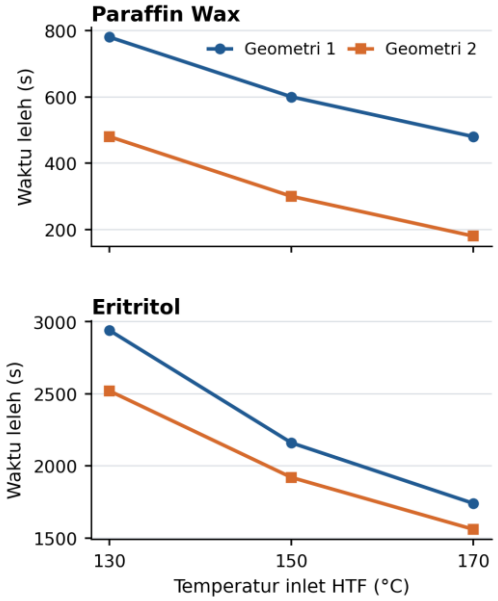


Figure 5. PCM melting time at HTF speed 3 m/s.

The outlet temperature of the CTF shows a very strong geometric influence. Geometry 1 produces *a narrow outlet* temperature, around 26.25-26.94 °C, so heat transfer to the cold fluid is still limited. Conversely, in Geometry 2, *the outlet* temperature approaches the *inlet* temperature of HTF, which is around 129-130 °C, 148.72-150 °C, and 168.51-170 °C depending on the operating level. These results confirm that *multi-CTF* not only accelerates PCM melting but also improves the system's ability to transfer heat to cold loads.

The graph of the CTF outlet temperature simulation at a speed of 3 m/s is presented in Figure 6.

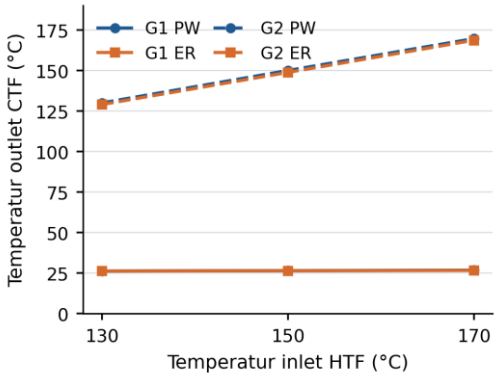


Figure 6. CTF outlet temperature at HTF velocity 3 m/s (PW: Paraffin Wax; ER: Erythritol).

PCM efficiency in Geometry 1 was 93.53-95.04% for *Paraffin Wax* and 96.17-96.55% for Erythritol. In Geometry 2, efficiency increased to nearly 100% for *Paraffin Wax* and 99.12-99.23% for Erythritol. This increase occurred because the distribution of the CTF pipe enlarged the heat transfer area, reduced *thermal dead zones*, and made the energy supplied by HTF more effectively absorbed by PCM.

The efficiency trends of the two PCMs for each geometry are shown in Figure 7.

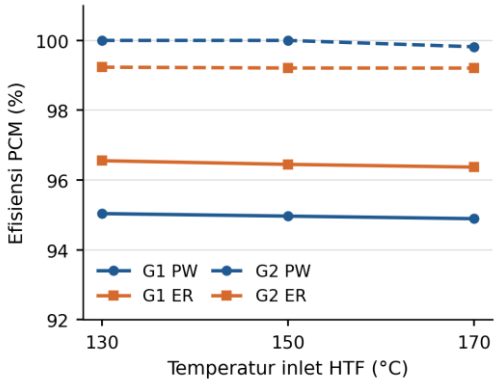


Figure 7. PCM efficiency at HTF speed 3 m/s.

Table 5. CTF *outlet* temperature and PCM efficiency

Indicator	Range of results and scientific significance
Outlet CTF G1	26,25-26,94 °C; heat transfer to CTF is limited by the contact area of a single CTF
Outlet CTF G2	129-170 °C; temperature approaches HTF level because

Indicator	Range of results and scientific significance
	thermal contact is more evenly distributed
Efisiensi PW G1	93,53-95,04%; increases with speed, but is limited by geometry
Efisiensi PW G2	98,82-100%; Highest performance and suitable for fast response
Efisiensi ER G1	96,17-96,55%; stable due to high latent heat
Efisiensi ER G2	99,12-99,23%; High and stable efficiency

The effect of HTF speed is more clearly seen in Geometry 1 compared to Geometry 2. In Geometry 1, the increase in velocity from 1 to 3 m/s increases forced convection, thereby slightly improving efficiency and *melting* rate. In Geometry 2, the system's response is relatively constant to velocity because the increased contact area and equalization of the heat path have made the heat transfer mechanism more optimal. In other words, after the geometric resistance is reduced, operating temperature becomes a more dominant parameter than flow velocity.

The stored thermal energy increases with the rise in the *inlet* temperature of the HTF. In *Paraffin Wax*, the energy ranges from 2666.03 to 2714.07 kJ at 130 °C, 3180.04 to 3234.58 kJ at 150 °C, and 3690.21 to 3754.21 kJ at 170 °C. For erythritol, the energy ranges from 1576.99 to 1580.66 kJ, 1877.26 to 1881.84 kJ, and 2177.71 to 2183.07 kJ for the same temperature levels. The energy values in Geometry 1 and 2 are identical because the PCM mass and temperature range are the same; the difference in geometry mainly affects the process speed, not the maximum capacity.

The relationship between HTF inlet temperature and stored thermal energy at a velocity of 3 m/s is shown in Figure 8.

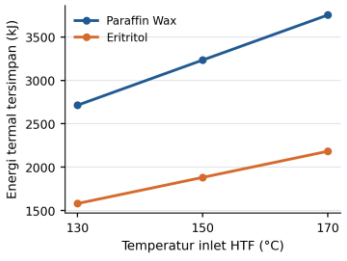


Figure 8. Thermal energy is stored at an HTF velocity of 3 m/s (G1 and G2 identical).

Compared to previous studies on *LHTES spiral coils* and *multi-tube* [15], [17], these findings reinforce that geometry with a larger contact area improves melting kinetics. *The novelty of* this study lies in the simultaneous comparison between single CTF and multi-CTF in *shell-and-spiral* TES with two PCMs with different characteristics. The results show that *multi-CTF* configuration is a more effective design strategy than simply increasing HTF speed, especially for applications that require short *charging* times.

Table 6. Summary of stored thermal energy

PCM and HTF temperature	Stored thermal energy (kJ)
Paraffin Wax 130 °C	2666,03-2714,07
Paraffin Wax 150 °C	3180,04-3234,58
Paraffin Wax 170 °C	3690,21-3754,21
Eritritol 130 °C	1576,99-1580,66
Eritritol 150 °C	1877,26-1881,84
Eritritol 170 °C	2177,71-2183,07

Table 7. Design implications based on simulation results

Design aspects	Recommendations and reasons
Fastest *charging* response	Geometri 2 + *Paraffin Wax* + 170 °C + 3 m/s; *melting time* 180 s
Highest efficiency	Geometri 2 + *Paraffin Wax*; almost all variations reach 100%
Efficiency stability	Geometri 2 + Eritritol; efficiency 99,12-99,23%
Energy capacity	PCM and temperature are determined; geometry does not change the final capacity
Parameter dominan	HTF geometry and temperature; HTF velocity has a secondary effect

In terms of temperature distribution, Geometry 2 shows the characteristics of multicenter heat transfer. Each CTF pipe acts as a thermal boundary that shortens the heat diffusion distance within the PCM. This condition reduces local heat accumulation around the spiral pipe and

accelerates the formation of a liquid zone throughout the volume. In Geometry 1, part of the PCM is farther from the heat exchange surface, thus remaining in the *mushy zone* longer. This difference explains why the final energy capacity can be the same, but the timing of achievement varies greatly.

The performance differences *between Paraffin Wax* and Erythritol can be understood from the relationship between melting point, latent heat, and operating temperature range. At HTF temperature 130 °C, *Paraffin Wax* is already far above its melting point, so the incoming energy is immediately used for melting and heating the liquid. Erythritol, on the other hand, requires greater sensitive heating before reaching about 119 °C. Therefore, the initial rate *of* liquid fraction of Erythritol, which is slower, is slower even though the material has a high latent storage potential.

An increase in HTF temperature from 130 to 170 °C has a stronger effect than an increase in flow velocity. Physically, temperature increases the *driving force* of heat transfer between HTF and PCM. Speed increase does increase the convection coefficient, but once the dominant resistance is in PCM, speed increase is not always followed by a comparable performance increase. This phenomenon aligns with the *multi-tube* LHTES findings stating that the increase in flow rate becomes less significant when the main resistance shifts to PCM.

From the outlet temperature side of the CTF, the performance spike in Geometry 2 should be interpreted as a consequence of a much larger thermal contact area. The five CTF pipes provide a more even interaction area between the liquid PCM and the cold fluid. This result is important for water heating applications, as *the outlet* temperature is a direct indicator of the system's load-bearing capability. In Geometry 1, the *constant outlet* temperature of about 26 °C indicates that the stored heat has not been effectively extracted by a single central pipe during the same simulation period.

PCM efficiency approaching 100% in Geometry 2 shows that geometric changes can reduce performance loss due to internal temperature inconsistency. However, efficiency values should not be interpreted separately from *pressure drop* and pump power requirements. *Multi-CTF* configurations are likely to add manufacturing complexity and flow resistance on the CTF side. Therefore, the best design for real applications needs to combine thermal performance, fabrication costs, pressure drop, and cyclic operation reliability.

The identical stored thermal energy in both geometries emphasizes an important concept in TES design. The geometry *of the heat exchanger* primarily regulates the rate of heat transfer, while the maximum capacity is determined by the mass of the PCM, latent heat, specific heat, and temperature range. Thus, the capacity enhancement strategy must be carried out through PCM selection, effective mass enhancement, or expansion of the operating range. Conversely, the most effective time response enhancement strategy is carried out through geometry optimization and heat transfer intensification.

Overall, the combination of Geometry 2 and *Paraffin Wax* at HTF 170 °C and 3 m/s produced the most responsive performance. This combination is recommended if the main target is short *charging* times. For applications requiring storage at higher temperatures and more stable heat dissipation, erythritol remains attractive despite requiring longer *melting times*. Final selection should consider the load profile and operating temperature of the application.

CONCLUSION

This study proves that CTF geometry configuration significantly affects the performance of PCM-based latent TES. Through *transient* CFD simulation with *an enthalpy-porosity* model, Geometry 2 using five CTF pipes produced a more even temperature distribution, *faster fluid fraction* development, *higher CTF outlet temperature, and better PCM efficiency compared to Geometry 1. Under the best conditions,* the melting time of Paraffin Wax *decreased from 480 s to 180 s, while Erythritol decreased from 1740 s to 1560 s. Paraffin wax* is more suitable for applications requiring rapid thermal response, while erythritol is more suitable for higher temperature applications requiring energy storage stability. The novelty of this article is proof that changes in CTF configuration in *the shell-and-spiral* TES are more dominant in heat transfer kinetics compared to increased HTF velocity. Further research needs to verify the results experimentally, test repeated charging-discharging cycles, analyze *pressure drop* and pump power consumption, and explore the use of *nano-PCM* or CTF pipe position optimization.

REFERENCES

[1] Z. Liu, Y. Liu, B. J. He, W. Xu, G. Jin, and X. Zhang, “Application and suitability analysis of the key technologies in nearly zero energy buildings in China,” Renewable and Sustainable Energy Reviews, 2019, doi: 10.1016/j.rser.2018.11.023.

[2] J. L. Holechek, H. M. E. Geli, M. N. Sawalhah, and R. Valdez, "A Global Assessment: Can Renewable Energy Replace Fossil Fuels by 2050?," Sustainability, vol. 14, no. 8, 2022, doi: 10.3390/su14084792.

[3] K. M. Kennedy et al., "The role of concentrated solar power with thermal energy storage in least-cost highly reliable electricity systems fully powered by variable renewable energy," Advances in Applied Energy, vol. 6, 2022, doi: 10.1016/j.adapen.2022.100091.

[4] E. Oro, A. de Gracia, A. Castell, M. M. Farid, and L. F. Cabeza, "Review on phase change materials (PCMs) for cold thermal energy storage applications," Applied Energy, 2012, doi: 10.1016/j.apenergy.2012.03.058.

[5] D. K. Yadav, P. K. S. Rathore, R. K. Singh, A. K. Gupta, and B. S. Sikarwar, "Experimental Study on Paraffin Wax and Soya Wax Supported by High-Density Polyethylene and Loaded with Nano-Additives for Thermal Energy Storage," Energies, vol. 17, no. 11, 2024, doi: 10.3390/en17112461.

[6] H. Nazir et al., "Recent developments in phase change materials for energy storage applications: A review," International Journal of Heat and Mass Transfer, 2019, doi: 10.1016/j.ijheatmasstransfer.2018.09.126.

[7] H. Mousa, J. Naser, and O. Houche, "Using PCM as energy storage material in water tanks: Theoretical and experimental investigation," Journal of Energy Storage, vol. 22, pp. 1-7, 2019, doi: 10.1016/j.est.2019.01.018.

[8] V. Saydam, M. Parsazadeh, M. Radeef, and X. Duan, "Design and experimental analysis of a helical coil phase change heat exchanger for thermal energy storage," Journal of Energy Storage, vol. 21, pp. 9-17, 2019, doi: 10.1016/j.est.2018.11.006.

[9] E. Privitera, R. Caponetto, F. Matera, and S. Vasta, "Impact of Geometry on a Thermal-Energy Storage Finned Tube during the Discharging Process," Energies, vol. 15, no. 21, 2022, doi: 10.3390/en15217950.

[10] B. M. S. Punniakodi and R. Senthil, "Experimental study on melting enhancement of phase change material in a vertical cylindrical latent heat storage using a short concentric helical heat transfer tube," Journal of Energy Storage, vol. 41, 2021, doi: 10.1016/j.est.2021.102879.

[11] A. Sole, H. Neumann, S. Niedermaier, I. Martorell, P. Schossig, and L. F. Cabeza, "Stability of sugar alcohols as PCM for thermal energy storage," Solar Energy Materials and Solar Cells, vol. 126, pp. 125-134, 2014, doi: 10.1016/j.solmat.2014.03.020.

[12] S. N. Gunasekara, R. Pan, J. N. Chiu, and V. Martin, "Polyols as phase change materials for surplus thermal energy storage," Applied Energy, vol. 162, pp. 1439-1452, 2016, doi: 10.1016/j.apenergy.2015.03.064.

[13] D. N. Bolmatenkov, M. I. Yagofarov, A. A. Sokolov, M. A. Ziganshin, and B. N. Solomonov, "The heat capacities and fusion thermochemistry of sugar alcohols," Journal of Molecular Liquids, vol. 330, 2021, doi: 10.1016/j.molliq.2021.115545.

[14] A. Dabestani and M. Kahani, "CFD analysis of rotation effect on flow patterns and heat transfer enhancement in a horizontal spiral tube heat exchanger," Case Studies in Thermal Engineering, vol. 64, 2024, doi: 10.1016/j.csite.2024.105494.

[15] M. M. Joybari, S. Seddegh, X. Wang, and F. Haghighat, "Experimental investigation of multiple tube heat transfer enhancement in a vertical cylindrical latent heat thermal energy storage system," Renewable Energy, vol. 140, pp. 234-244, 2019, doi: 10.1016/j.renene.2019.03.037.

[16] D. J. Jasim, S. H. H. Karouei, T. J. Mohammed, and A. S. Al-Shati, "Hydrothermal behaviour of hybrid nanofluid flow in two types of shell and helical coil tube heat exchangers with a new design," International Journal of Thermofluids, vol. 24, 2024, doi: 10.1016/j.ijft.2024.100902.

[17] C. Chen, H. Zhang, X. Gao, T. Xu, Y. Fang, and Z. Zhang, "Numerical and experimental investigation on latent thermal energy storage system with spiral coil tube and paraffin/expanded graphite composite PCM," Energy Conversion and Management, vol. 126, pp. 889-897, 2016, doi: 10.1016/j.enconman.2016.08.068.

[18] H. H. Noor et al., "Numerical evaluation of the influence of various fluid types on the efficiency of distinctively designed shell-and-spiral tube heat exchangers," Case Studies in Thermal Engineering, vol. 76, 2025, doi: 10.1016/j.csite.2025.107226.

[19] S. Sokakini, J. V. Simo Tala, L. Nadau, A. Ilinca, and D. Bougeard, "Heat transfer enhancement in shell and tube Latent Heat Thermal Energy Storage units for waste heat recovery applications," Applied Thermal Engineering, vol. 274, 2025, doi: 10.1016/j.applthermaleng.2025.126564.

[20] J. Guo, C. Tan, Y. Jin, J. Zhao, and Z. Liu, "A novel solar-active integrated biobased facade system for enhanced thermal storage, energy efficiency, and climate adaptability," Energy

Conversion and Management, vol. 349, 2026, doi: 10.1016/j.enconman.2025.120851.

[21] A. Da Col, F. Bentivoglio, and B. Stutz, "Thermal modelling of the discharge of a 180 kW h latent thermal energy storage demonstrator," Journal of Energy Storage, vol. 144, 2026, doi: 10.1016/j.est.2025.119689.

[22] Y. Huang, A. Stonehouse, and C. Abeykoon, "Encapsulation methods for phase change materials - A critical review," International Journal of Heat and Mass Transfer, 2023, doi: 10.1016/j.ijheatmasstransfer.2022.123458.

[23] A. S. S. Bilal et al., "Enhancing thermo-physical properties of paraffin wax phase change material with MXene nanoflakes," Results in Engineering, vol. 25, 2025, doi: 10.1016/j.rineng.2025.104557.

[24] G. Righetti et al., "Experimental investigation of high temperature organic phase change materials for waste heat recovery," International Journal of Thermofluids, vol. 28, 2025, doi: 10.1016/j.ijft.2025.101293.

[25] Z. Ahcin, A. Kitanovski, and J. Tusek, "Latent thermal energy storage using solid-state phase transformation in caloric materials," Cell Reports Physical Science, 2024, doi: 10.1016/j.xcrp.2024.102175.

[26] W. Delgado-Diaz et al., "Optimization of hybrid sensible-latent seasonal heat storage systems," Applied Energy, vol. 399, 2025, doi: 10.1016/j.apenergy.2025.126235.

[27] X. Jin et al., "Experimental investigation of the novel melting point modified Phase-Change material for heat pump latent heat thermal energy storage application," Energy, vol. 216, 2021, doi: 10.1016/j.energy.2020.119191.

[28] P. R. Chakraborty, "Enthalpy porosity model for melting and solidification of pure-substances with large difference in phase specific heats," International Communications in Heat and Mass Transfer, vol. 81, pp. 183-189, 2017, doi: 10.1016/j.icheatmasstransfer.2016.12.023.

[29] Z. Piran, S. S. M. Ajarostaghi, and M. Farhadi, "Impact of employing twisted tube with spiral V-shaped axial fins on the charging performance inside a phase change material storage," Journal of Energy Storage, vol. 100, 2024, doi: 10.1016/j.est.2024.113645.

[30] N. Sohrabi, R. Haddadvand, and H. Nabi, "Numerical investigation of fluid nanohybrid type and volume concentration on heat transfer and pressure drop in spiral double tube heat exchanger," Case Studies in Thermal Engineering, vol. 60, 2024, doi: 10.1016/j.csite.2024.104751.

[31] M. A. Faisal, A. Rahmani, and M. Akrami, "Numerical Investigation of Solar Collector Performance with Encapsulated PCM: A Transient, 3D Approach," Energies, vol. 17, no. 21, 2024, doi: 10.3390/en17215243.

[32] A. R. Mazhar, S. Liu, and A. Shukla, "Numerical investigation of heat transfer enhancement using corrugated pipes in a PCM for grey water harnessing," Thermal Science and Engineering Progress, vol. 23, 2021, doi: 10.1016/j.tsep.2021.100909.

[33] M. K. Fahad, M. J. Hasan, N. F. Ifraj, and D. C. Dey, "Numerical investigation on different design arrangements of helical heat exchangers with varying cross-sections utilizing ternary hybrid nanofluids," Heliyon, vol. 10, no. 14, 2024, doi: 10.1016/j.heliyon.2024.e34481.

[34] Q. Gong, C. Yu, W. Wang, and Y. Wang, "Experimental and numerical exploration on improved heat transfer by continuous spiral flow in shell of spiral wound corrugated tube heat exchanger," Case Studies in Thermal Engineering, vol. 51, 2023, doi: 10.1016/j.csite.2023.103483.

[35] N. Ben Ali et al., "Numerical exploration of the impact of fluid type in a uniquely designed shell and spiral tube heat exchanger," Case Studies in Thermal Engineering, vol. 61, 2024, doi: 10.1016/j.csite.2024.104798.

[36] E. Paroutoglou et al., "A Numerical Parametric Study of a Double-Pipe LHTES Unit with PCM Encapsulated in the Annular Space," Sustainability, vol. 14, no. 20, 2022, doi: 10.3390/su142013317.